23BU006 BL-9B

Ultrafast Spin-Dependent Dynamics in a Carrier-Tuned Topological Insulator

K. Sumida[a], K. Kunitomo[b], M. Kakoki[b], K. A. Kokh[c], O. E. Tereshchenko[c], J. Reimann[d], J. Güdde[d], U. Höfer[d], K. Miyamoto[a], T. Okuda[a,e], and A. Kimura[b,e]

[a]*Hiroshima Synchrotron Radiation Center, Hiroshima University, 2-313 Kagamiyama, Higashi-Hiroshima 739-0046, Japan*
[b]*Graduate School of Advanced Science and Engineering, Hiroshima University, 1-3-1 Kagamiyama, Higashi-Hiroshima 739-8526, Japan*
[c]*Physics Department, Novosibirsk State University, ul. Pirogova 2, 630090 Novosibirsk, Russia*
[d]*Department of Physics and Materials Sciences Center, Philipps-University, D-35032 Marburg, Germany*
[e]*International Institute for Sustainability with Knotted Chiral Meta Matter (SKCM²), 1-3-1 Kagamiyama, Higashi-Hiroshima 739-8526, Japan*

Keywords: Topological insulator, Time-resolved ARPES, Spin-resolved ARPES, Ultrafast carrier dynamics, Spin texture.

Topological insulators (TIs) characterized by spin-polarized Dirac-cone-like band structures on their surfaces have been extensively investigated over the last decade. As a hallmark of TIs caused by strong spin-orbit coupling, the spin-momentum-locked topological surface state (TSS) offers a pure spin current on their surfaces. The spin-polarized surface electrons of TIs are robust against nonmagnetic impurities and defects. So far, many TIs, such as Bi_2Se_3, Bi_2Te_3, and Sb_2Te_3, have been theoretically predicted and experimentally verified by angle-resolved photoemission spectroscopy (ARPES) with spin-resolution.

Recently, the ultrafast optical response of TSS has attracted much attention. Time-resolved ARPES utilizing femtosecond-laser reveals several characteristics and functionalities, *e.g.*, the emergence of Floquet state [1], population inversion [2], and the surface photovoltage effect [3]. However, the ultrafast carrier dynamics derived from the unique spin texture of TSS have hardly been investigated.

In this work, we investigated the spin-dependent ultrafast surface carrier dynamics of a ternary topological insulator $(Sb,Bi)_2Te_3$, where the Dirac point is adjusted to the Fermi energy (E_F), by a combination of laser-based time-resolved ARPES and synchrotron-based spin-resolved ARPES techniques. The pump-probe time-resolved ARPES measurements were performed at Philipps University of Marburg. We used two different pump energies: mid-infrared (MIR) at 0.30 eV and visible (VIS) at 2.58 eV [Figs. 1(a) and 1(d)]. We used an ultraviolet (UV) at 5.16 eV light as the probe. The spin-resolved ARPES measurements, utilizing very low energy electron diffraction type spin-polarimeters, were performed at ESPRESSO end-station (BL-9B) of Hiroshima Synchrotron Radiation Center [4].

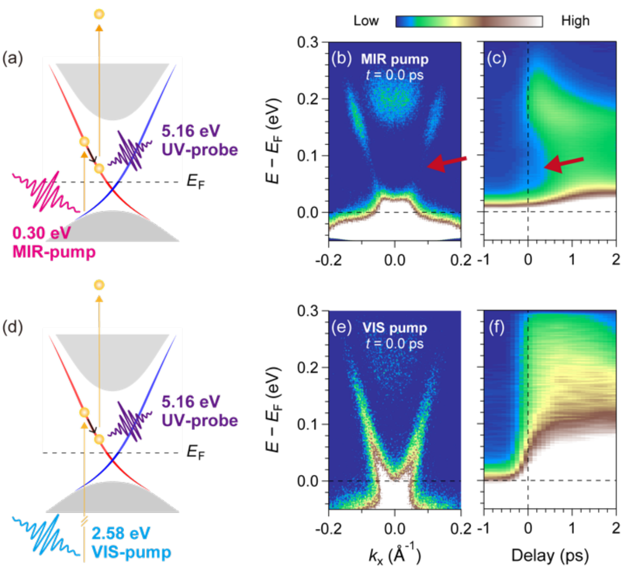

FIGURE 1. (a) Schematic illustration of time-resolved ARPES experiment using MIR-pump and UV-probe. (b) ARPES image of $(Sb_{0.57}Bi_{0.43})_2Te_3$ along $\bar{\Gamma}-\bar{K}$ direction recorded at t = 0 ps. (c) Photoemission intensity profile as a function of delay time. (d-f) Same as (a-c) but using VIS-pump.

Figure 1(b) shows the ARPES image recorded at temporal overlap (t = 0 ps) with the MIR-pump. We can recognize the Dirac-cone-like TSS and bulk conduction band above E_F. We also notice that the photoemission intensities at the TSS in a certain energy region around 0.05 eV are very weak [see the red arrow in Fig. 1(b)], while those around 0.15 eV are pronounced. To illustrate the temporal evolution of the bands, Figure 1(c) displays the momentum-integrated photoemission intensity profile as a function of delay time. We find a dip structure around 0.05 eV from 0.0 to 0.5 ps. After 0.5 ps, the intensity around 0.05 eV drastically increases because the photo-excited electrons at higher energy states relax through intra-band and inter-band scatterings. These findings suggest that the direct transition is prohibited around 0.05 eV in the MIR-pump scheme. To compare the ultrafast carrier dynamics, we also performed time-resolved ARPES using the VIS-pump [Figs. 1(e) and 1(f)]. However, in sharp contrast to the MIR-pump scheme, no dip structures are visible at $t = 0$ ps.

Since the forbidden transition observed in the MIR-pump scheme likely stems from the unique spin texture of the TSS, we proceeded with the spin-resolved measurement of the occupied bands below E_F. Figure 2(a) shows the spin-resolved ARPES image captured at 17.0 eV. Red and blue colors correspond to positive and negative in-plane spin-polarization, respectively. From E_F to -0.3 eV, the spin-polarized lower portion of TSS is evident. Additionally, M-shaped spin-split Rashba bands are observed around -0.5 eV. Since the directions of in-plane spin-polarization at the upper and lower TSSs are reversed with respect to the Dirac point, the forbidden transitions in the "resonant" MIR-pump scheme are most likely caused by the intrinsic spin texture of TSS, as depicted in Fig. 2(b). In the VIS-pump scheme, on the other hand, the direct transition to the upper TSS is allowed because the transition occurs from the unpolarized deeper-lying bulk continuum states. Finally, we discuss why the direct transition is permitted around 0.15 eV at the TSS in the MIR-pump scheme [Fig. 1(b)]. The upper panels of Fig. 2(c) show the constant energy contours recorded at $t \sim 0$ ps with VIS-pump. At 0.05 eV, an isotropic shape contour is seen. On the other hand, at 0.15 eV, the contour shape undergoes deformation from circular to hexagonal due to the warping effect. On the warped bands, it is known that not only in-plane but also out-of-plane spin components emerge [the lower panels of Fig. 2(c)] [5]. In such a case, the direct transition would be partially allowed.

In conclusion, we have experimentally demonstrated the spin-dependent forbidden transition in the TI by using time-resolved ARPES and spin-resolved ARPES. Our findings pave the way for ultrafast opto-spintronic applications using the TSS of TIs.

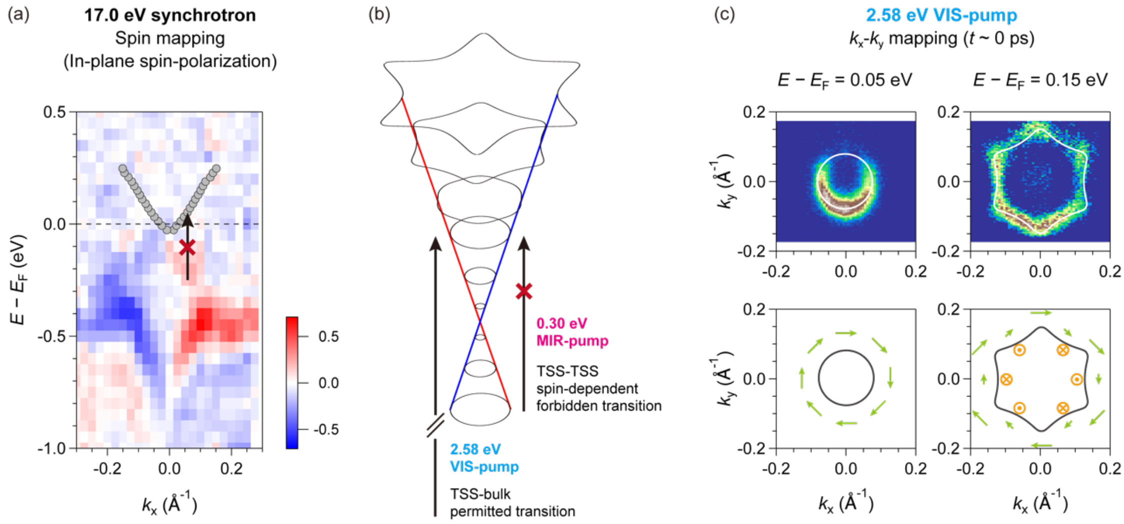

FIGURE 2. (a) In-plane spin-polarization mapping of $(Sb_{0.57}Bi_{0.43})_2Te_3$ along $\bar{\Gamma}-\bar{K}$ direction recorded at 17.0 eV. Gray circles represent the fitting results of the TSS shown in Fig. 1(e). (b) Schematic illustration of spin-dependent direct transition using MIR- and VIS-pump schemes. (c) Upper panel: constant energy contours at 0.05 and 0.15 eV recorded at $t \sim 0$ ps with VIS-pump. Lower panel: Schematic illustrations of spin texture of isotropic (left) and anisotropic TSS (right). Light green and orange colors correspond to the in-plane and out-of-plane spin components, respectively.

REFERENCES

1. Y. H. Wang *et al.,* Science **342**, 453 (2013).
2. S. Y. Zhu *et al.,* Sci. Rep. **5**, 13213 (2015)., K. Sumida *et al*., Phys. Rev. B **99**, 085302 (2019).
3. K. Sumida *et al*., Sci. Rep. **7**, 14080 (2017)., T. Yoshikawa *et al*., Phys. Rev. B **100**, 165311 (2019).
4. T. Okuda *et al.,* Rev. Sci. Instrum. **82**, 103302 (2011).
5. L. Fu, Phys. Rev. Lett. **103**, 266801 (2009)., S. Souma *et al*., Phys. Rev. Lett. **106**, 216803 (2011).